

# NUNO: A General Framework for Learning Parametric PDEs with Non-Uniform Data

Songming Liu, Zhongkai Hao, Chengyang Ying,  
Hang Su, Ze Cheng, Jun Zhu





# Background



# Neural Operator

## ◆ Parameterized PDEs

$$F_a(u(x), x) = 0$$

$a(y) \in \mathcal{A}, y \in \Omega_a$  is the parameter function (e.g., bias term of the boundary condition)

$u(x) \in \mathcal{U}, x \in \Omega_u$  is the unknown solution

## ◆ Training neural operators

◆ To approximate the operator  $G^\dagger: \mathcal{A} \rightarrow \mathcal{U}$  with a neural model  $f_\theta$

◆ Data-driven training with a dataset  $\{(a_j, u_j)\}_{j=1}^N$ , where  $a \sim \mu$

$$\min_{\theta \in \Theta} \mathbb{E}_{a \sim \mu} \|f_\theta(a) - u\|$$



# Neural Operator

## ◆ Parameterized PDEs

$$F_a(u(x), x) = 0$$

$a(y) \in \mathcal{A}, y \in \Omega_a$  is the parameter function (e.g., bias term of the boundary condition)

$u(x) \in \mathcal{U}, x \in \Omega_u$  is the unknown solution

## ◆ Training neural operators

◆ To approximate the operator  $G^\dagger: \mathcal{A} \rightarrow \mathcal{U}$  with a neural model  $f_\theta$

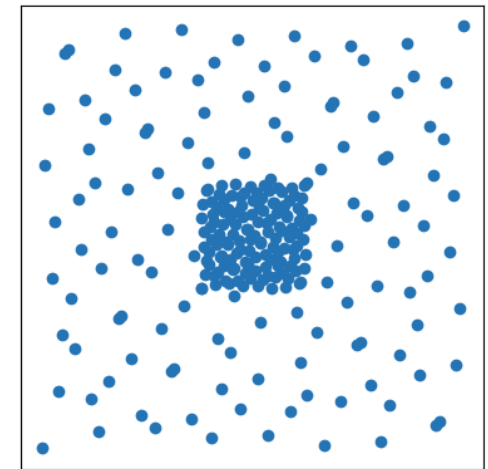
◆ Data-driven training with a dataset  $\{(a_j, u_j)\}_{j=1}^N$ , where  $a \sim \mu$

$$\min_{\theta \in \Theta} \mathbb{E}_{a \sim \mu} \|f_\theta(a) - u\|$$

# Challenge of Non-Uniform Data

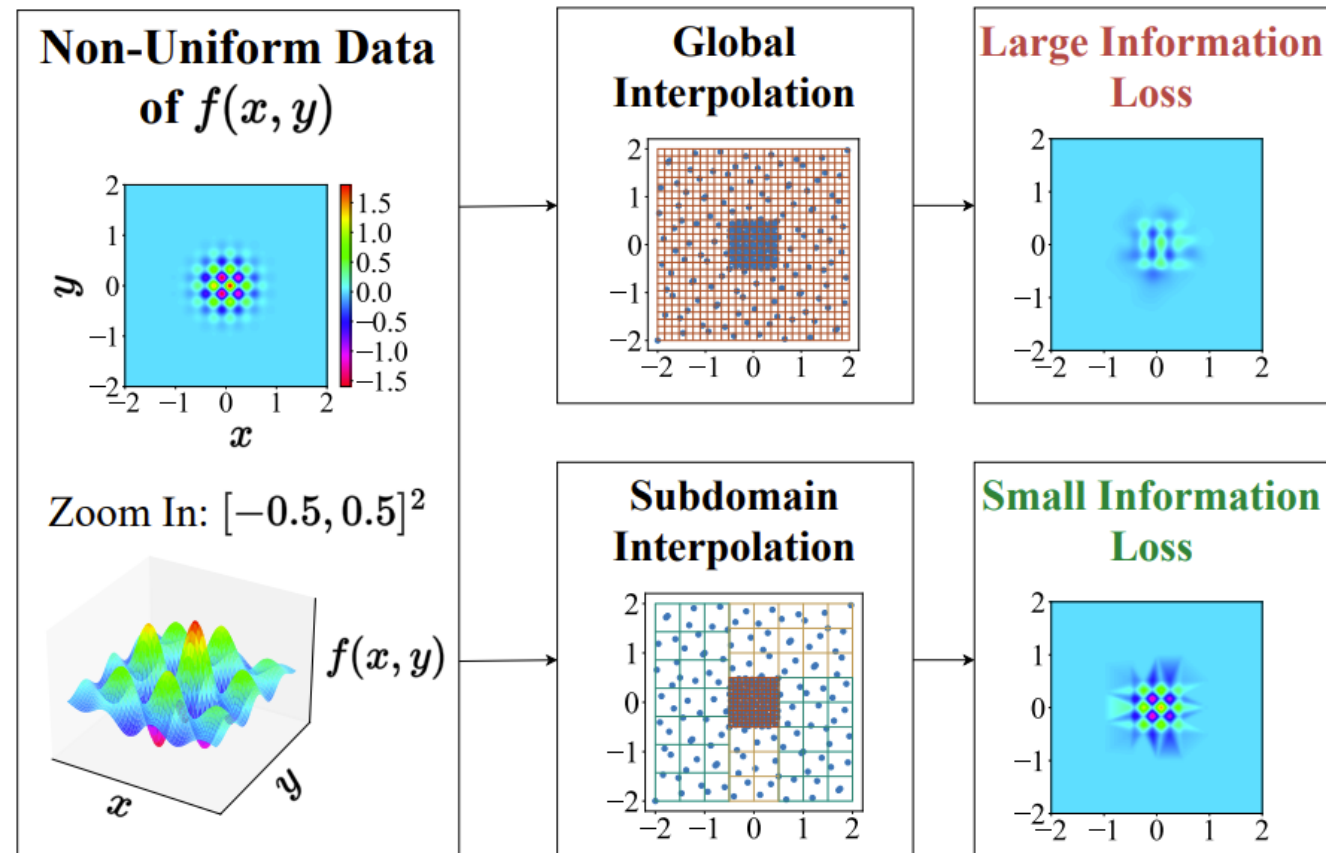
- ◆ **Our model  $f_\theta$** 
  - ◆ takes a **function**  $a(y)$  as input and
  - ◆ outputs another **function**  $u(x)$  as output
- ◆ **Representation of functions**
  - ◆ Point-cloud values,  $a := \{a(x^{(i)})\}_{i=1}^M$
- ◆ **Challenge**
  - ◆ Hard to extract features: efficiency, ...
  - ◆ Unable to employ **mesh-based** techniques, e.g., FFT, CNN, ...

Point cloud  $\{x^{(i)}\}_{i=1}^M$



# Interpolation Error

- ◆ Interpolation from point cloud to uniform grids

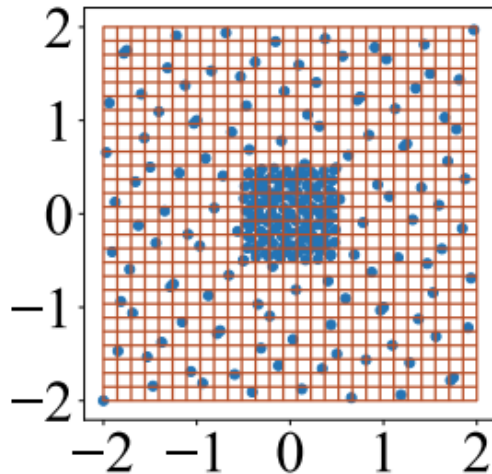




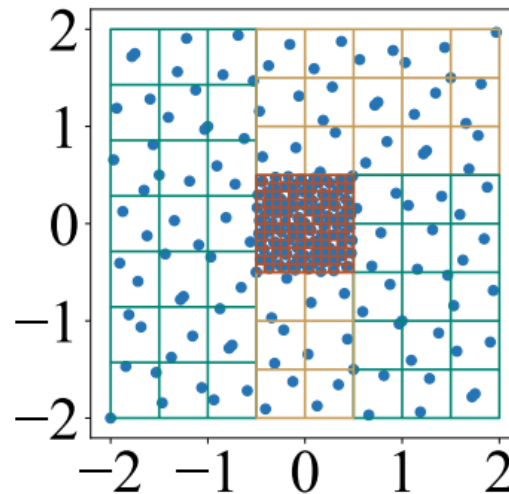
# Method

# Subdomain Interpolation

## Global Interpolation



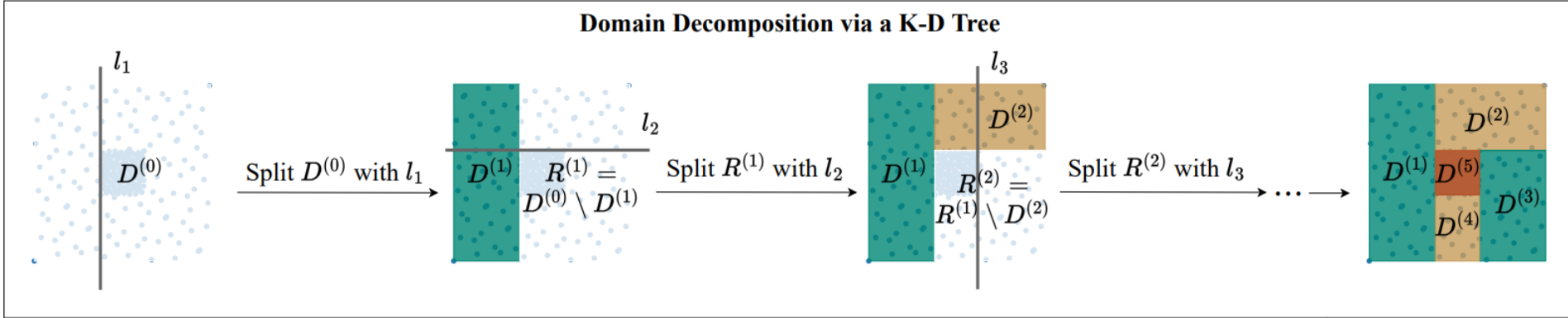
## Subdomain Interpolation



- ◆ Divide the domain into several **subdomains**
- ◆ Interpolation over each subdomain **separately**
- ◆ Adaptively apply **coarse** uniform grids on **sparse** subdomains and **fine** grids on **dense** ones



# K-D Tree Domain Decomposition



## Algorithm 1 Domain Decomposition via a K-D Tree

- 1: **Input:** initial point cloud  $D^{(0)}$  and the number of sub-point clouds  $n$
- 2: **Output:** a set of sub-point clouds  $\mathcal{S}$
- 3: **Initialize:**  $\mathcal{S} \leftarrow \{D^{(0)}\}$
- 4: **repeat**
- 5:   Choose  $D^* = \arg \max_{D \in \mathcal{S}} (|D| \cdot \text{KL}(P \parallel Q; D))$
- 6:    $\mathcal{S} \leftarrow \mathcal{S} - \{D^*\}$
- 7:   Select the dimension  $k$ ,  $1 \leq k \leq d$ , where the bounding box of  $D^*$  has the largest scale
- 8:   Determine the hyperplane  $x_k = b^*$ , where  $b^* = \arg \max_{b \in \mathcal{B}} \text{Gain}(D^*, b)$  and  $\mathcal{B}$  is a set of discrete candidates for  $b$
- 9:   Partition  $D^*$  with  $x_k = b^*$
- 10:    $\mathcal{S} \leftarrow \mathcal{S} \cup \{D^*_{x_k > b^*}, D^*_{x_k \leq b^*}\}$
- 11: **until**  $|\mathcal{S}| = n$

$$\text{KL}(P \parallel Q; D) := \sum_j \frac{|D_j|}{|D|} \ln \left( \frac{|D_j|}{|D|} \middle/ \frac{1}{\prod_{i=1}^d N_i} \right). \quad (4)$$

In calculating  $P$ , we employ histogram density estimation. Specifically, we divide the bounding box of  $D$  uniformly into  $N_1 \times \dots \times N_d$  cells, and  $D_j$  is defined as  $\{x \mid x \in D \wedge x \in \text{the } j\text{-th cell}\}$ , for  $1 \leq j \leq \prod_{i=1}^d N_i$ .

$$\begin{aligned} \text{KL}(P \parallel Q; D^*) &= \frac{|D^*_{x_k > b}|}{|D^*|} \text{KL}(P \parallel Q; D^*_{x_k > b}) \\ &\quad - \frac{|D^*_{x_k \leq b}|}{|D^*|} \text{KL}(P \parallel Q; D^*_{x_k \leq b}), \end{aligned} \quad (5)$$

where  $D^*_{x_k > b}$ ,  $D^*_{x_k \leq b}$  are defined as  $\{x \mid x \in D^* \wedge x_k > b\}$  and  $\{x \mid x \in D^* \wedge x_k \leq b\}$ , respectively.

# Overall Architecture

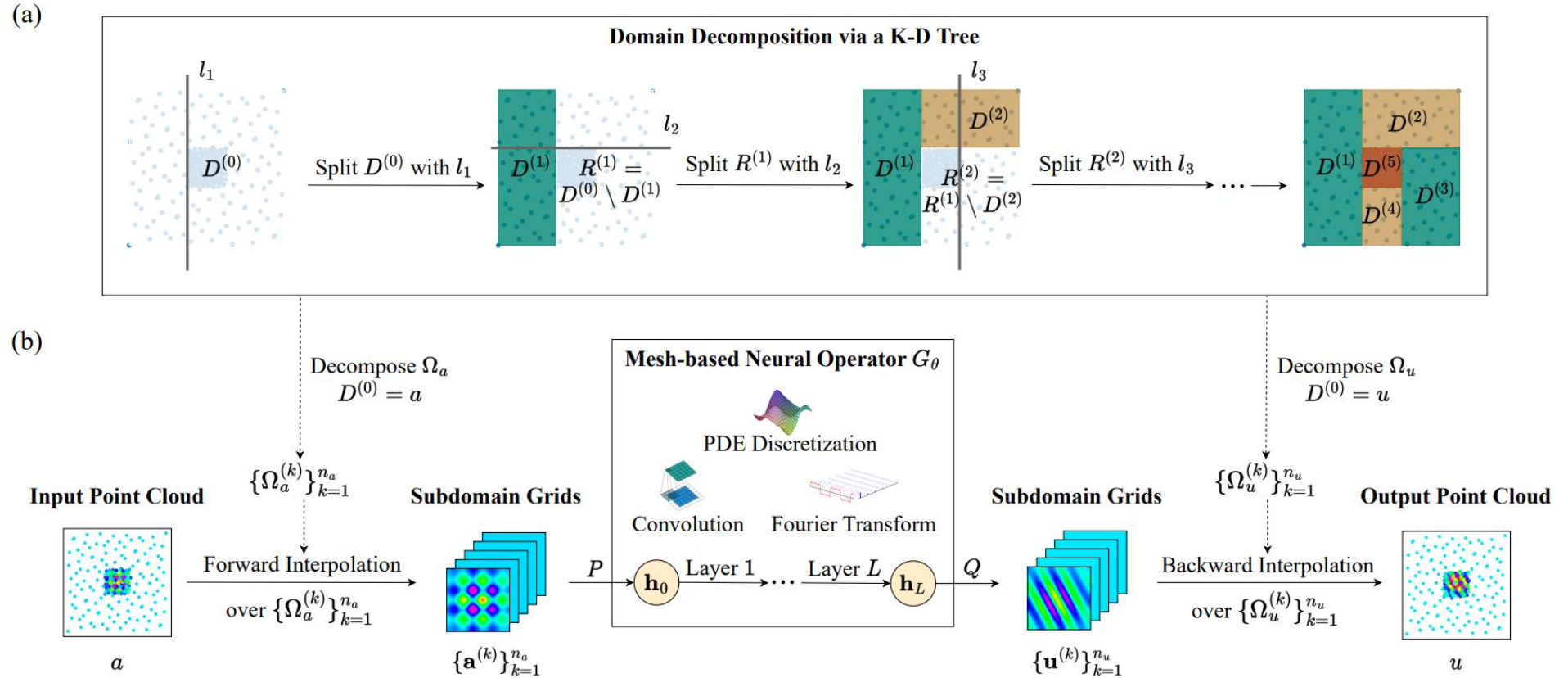


Figure 2: **(a) Domain decomposition:** starting from  $D^{(0)}$ , each time we choose to split a sub-point cloud with a hyperplane  $l_i$ . After 4 iterations, we obtain 5 sub-point clouds distributed more uniformly within their bounding boxes. **(b) NUNO framework:** 1. interpolation to subdomain grids; 2. projection by  $P$ ; 3. pass through the mesh-based neural operator with  $L$  layers ( $\mathbf{h}_0, \dots, \mathbf{h}_L$  indicate hidden embeddings of each layer); 4. projection by  $Q$ ; 5. interpolation back to the point cloud.



# Experiments



# Experiment Setup

- ◆ **Evaluation Metric:**

- ◆  $L^2$  Relative Error. We report the mean and 95% CI in 5 runs.

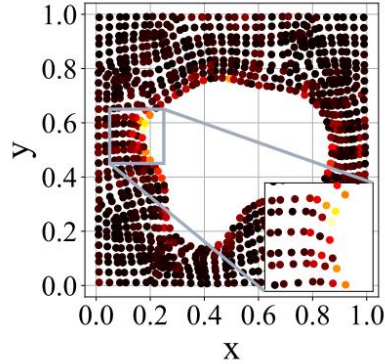
- ◆ **Baselines:**

- ◆ **Mesh-based Neural Operators:** U-Net<sup>[1]</sup>, FNO<sup>[2]</sup>, MWNO<sup>[3]</sup>, NU-NO (**ours**, “NU-FNO” indicates that our framework adopts an FNO as the underlying mesh-based model)
- ◆ **Mesh-less Neural Operators:** DeepONet<sup>[4]</sup>, GraphNO<sup>[5]</sup>, Geo-FNO<sup>[6]</sup>, PointNet<sup>[7]</sup>

- ◆ **Problems:**

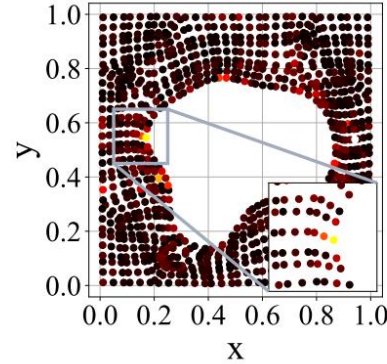
- ◆ 2D Elasticity, (2+1)D Channel Flow, 3D Heatsink

# 2D Elasticity



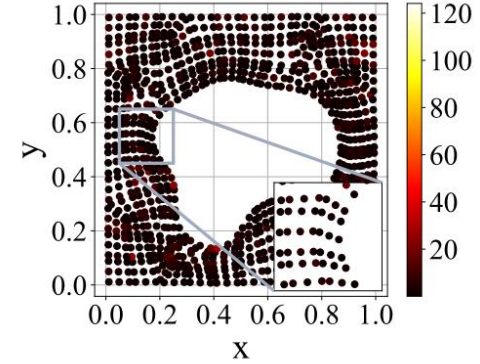
Mean Absolute Error: 7.76

(a) FNO (global interpolation)



Mean Absolute Error: 7.45

(b) Geo-FNO (learned)



Mean Absolute Error: **3.12**

(c) NU-FNO (**ours**)

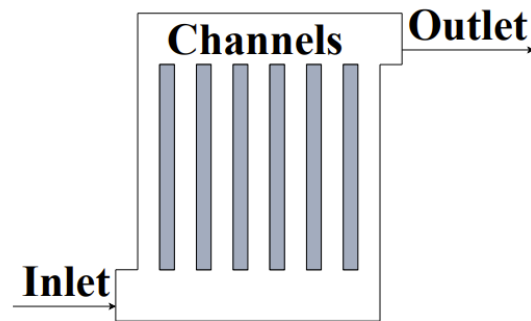
Table 1: Experimental results of 2D elasticity. R mesh and O mesh are adaptive meshes (Li et al., 2022).

Method	Mesh Size	Training Time		$L^2$ Relative Error ( $\times 10^{-2}$ )	
		per Epoch	per Run	Training	Testing
NU-FNO ( <b>ours</b> )	1024 <sup>1</sup>	2.3 s	19.6 min	<b>1.68 <math>\pm</math> 0.08</b>	<b>1.93 <math>\pm</math> 0.11</b>
FNO (global interpolation)	1681	<b>1.2 s</b>	<b>9.7 min</b>	3.41 $\pm$ 0.08	6.16 $\pm$ 0.16
U-Net (global interpolation)	1681	2.3 s	18.8 min	1.74 $\pm$ 0.02	6.82 $\pm$ 0.06
Geo-FNO (R mesh)	1681	1.7 s	14.2 min	3.53 $\pm$ 0.09	5.03 $\pm$ 0.09
Geo-FNO (O mesh)	1353	2.0 s	16.4 min	4.12 $\pm$ 0.16	4.28 $\pm$ 0.15
Geo-FNO (learned)	meshless	2.3 s	19.1 min	2.07 $\pm$ 0.99	4.31 $\pm$ 2.24
GraphNO	meshless	96.8 s	5.4 h	17.5 $\pm$ 1.26	16.9 $\pm$ 1.28
DeepONet	meshless	40.0 s	11.0 h	2.80 $\pm$ 0.13	12.0 $\pm$ 0.16

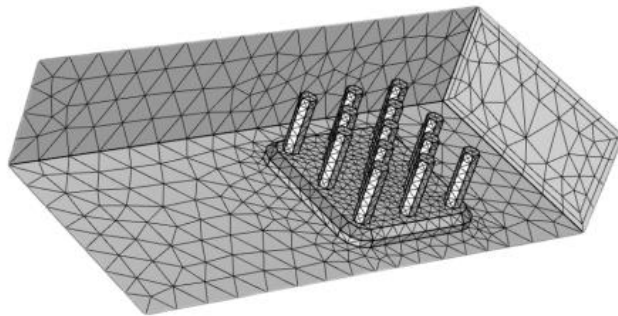
<sup>1</sup> In this paper, all mesh sizes mentioned for our method specifically refer to the *combined total number* of points across all subdomains, rather than the number of points within each individual subdomain.

# (2+1)D Channel Flow & 3D Heatsink

## ◆ (2+1)D channel flow



## ◆ 3D heatsink



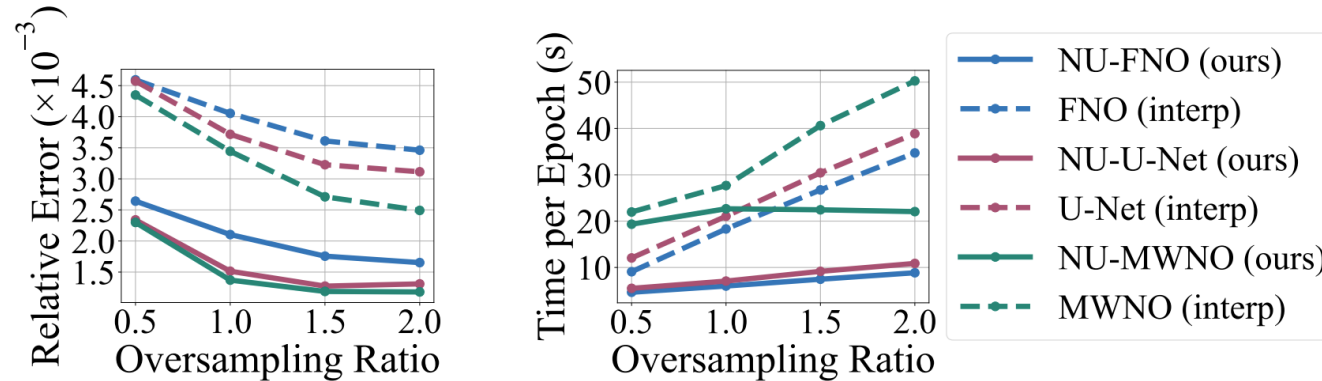
## ◆ $L^2$ relative error and training time per epoch

Methods	(2+1)D Channel flow		3D Heatsink	
	Error ( $\times 10^{-3}$ ) ↓	Time ↓	Error ( $\times 10^{-2}$ ) ↓	Time ↓
NU-FNO ( <b>ours</b> )	$1.74 \pm 0.05$	<b>7.2 s</b>	<b><math>5.09 \pm 0.48</math></b>	<b>4.7 s</b>
FNO (global interp)	$3.61 \pm 0.19$	26.9 s	$7.68 \pm 0.25$	6.2 s
NU-U-Net ( <b>ours</b> )	$1.27 \pm 0.03$	8.6 s	$6.31 \pm 0.31$	5.2 s
U-Net (global interp)	$3.29 \pm 0.15$	29.5 s	$8.27 \pm 0.14$	7.4 s
NU-MWNO ( <b>ours</b> )	<b><math>1.22 \pm 0.06</math></b>	22.9 s	$5.36 \pm 0.24$	18.3 s
MWNO (global interp)	$2.71 \pm 0.63$	40.6 s	$7.38 \pm 0.12$	21.0 s
Geo-FNO (learned)	$2.15 \pm 0.83$	114.9 s	-	-
GraphNO	$37.02 \pm 0.00$	193.6 s	-	-
DeepONet	$119.86 \pm 15.82$	235.8 s	-	-
PointNet	-	-	$56.42 \pm 27.60$	45.3 s



# Ablation Study

- How does the performance vary with **mesh size** and the **number of subdomains**?



	Method	Number of Subdomains			
		4	8	12	16
$L^2$ Rel. Err. ( $\times 10^{-3}$ ) Average	NU-FNO	1.92	1.71	1.31	<b>0.85</b>
	NU-U-Net	1.33	1.27	1.21	<b>0.88</b>
	NU-MWNO	1.23	1.19	1.06	<b>0.72</b>
Training Time per Epoch (s)	NU-FNO	9.5	7.2	6.7	<b>5.7</b>
	NU-U-Net	11.2	8.6	8.0	<b>6.9</b>
	NU-MWNO	27.6	23.9	23.1	<b>22.7</b>

**“Blessing of Subdomains”**



# References

- [1] Ronneberger, O., Fischer, P., and Brox, T. [U-net: Convolutional networks for biomedical image segmentation](#). In International Conference on Medical image computing and computer-assisted intervention, pp. 234–241. Springer, 2015.
- [2] Li, Z., Kovachki, N., Azizzadenesheli, K., Liu, B., Bhattacharya, K., Stuart, A., and Anandkumar, A. [Fourier neural operator for parametric partial differential equations](#). arXiv preprint arXiv:2010.08895, 2020a.
- [3] Gupta, G., Xiao, X., and Bogdan, P. [Multiwavelet-based operator learning for differential equations](#). Advances in Neural Information Processing Systems, 34:24048–24062, 2021.
- [4] Lu, L., Jin, P., Pang, G., Zhang, Z., and Karniadakis, G. E. [Learning nonlinear operators via deeponet based on the universal approximation theorem of operators](#). Nature Machine Intelligence, 3(3):218–229, 2021.





# References

- [5] Li, Z., Kovachki, N., Azizzadenesheli, K., Liu, B., Bhattacharya, K., Stuart, A., and Anandkumar, A. [Neural operator: Graph kernel network for partial differential equations](#). arXiv preprint arXiv:2003.03485, 2020b.
- [6] Li, Z., Huang, D. Z., Liu, B., and Anandkumar, A. [Fourier neural operator with learned deformations for pdes on general geometries](#). arXiv preprint arXiv:2207.05209, 2022.
- [7] Qi, C. R., Su, H., Mo, K., and Guibas, L. J. [Pointnet: Deep learning on point sets for 3d classification and segmentation](#). In Proceedings of the IEEE conference on computer vision and pattern recognition, pp. 652–660, 2017.



# Thank You!

Paper



Code

